Bioorganic & Medicinal Chemistry 18 (2010) 1321–1330

Contents lists available at ScienceDirect

Bioorganic & Medicinal Chemistry

journal homepage: www.elsevier.com/locate/bmc

Structure and in vitro antitumor activity evaluation of brominated diterpenes from the red alga *Sphaerococcus coronopifolius*

Vangelis Smyrniotopoulos [a], Constantinos Vagias [a], Céline Bruyère [b], Delphine Lamoral-Theys [c], Robert Kiss [b], Vassilios Roussis [a,*]

[a] Department of Pharmacognosy and Chemistry of Natural Products, School of Pharmacy, University of Athens, Panepistimiopolis Zografou, Athens 15771, Greece
[b] Université Libre de Bruxelles, Laboratoire de Toxicologie, Toxicologie et Chimie Physique Appliquée, Institut de Pharmacie, Boulevard du Triomphe, 1050 Bruxelles, Belgium
[c] Université Libre de Bruxelles, Laboratoire de Chimie Analytique, Toxicologie et Chimie Physique Appliquée, Institut de Pharmacie, Boulevard du Triomphe, 1050 Bruxelles, Belgium

ARTICLE INFO

Article history:
Received 13 October 2009
Revised 2 December 2009
Accepted 8 December 2009
Available online 16 December 2009

Keywords:
Sphaerococcus coronopifolius
Coronone
Sphaerostanol
10*R*-Hydroxy-bromocorodienol
Absolute stereochemistry
Brominated diterpenes
Antitumor activity

ABSTRACT

A novel bromoditerpene methyl ketone (**1**), two new bromoditerpene alcohols featuring a neodolastane (**2**), and a bromocorodienol skeleton (**3**), along with 13 previously reported metabolites (**4**–**16**) were isolated from the organic extract of *Sphaerococcus coronopifolius* collected from the rocky coasts of Corfu island in the Ionian Sea. The structures of the new natural products, as well as their relative stereochemistry, were elaborated on the basis of extensive spectral analysis, including 2D NMR experiments. The absolute stereochemistry of metabolite **3** was determined using the modified Mosher's method. The isolated metabolites were evaluated for their antitumoral activity against four human apoptosis-resistant (U373, A549, SKMEL-28, OE21) and two human apoptosis-sensitive (PC-3, LoVo) cancer cell lines with IC_{50} in vitro growth inhibitory concentrations in the range 3–100 μM.

1. Introduction

Cancer-related death will be ranked first in industrialized countries in 2015.[1] As long as a cancer has not yet metastasized surgery remains the treatment of choice for treating cancer patient because an apparent cure can be obtained by total tumor removal. In contrast, if the cancer has already metastasized by the time of diagnosis, adjuvant therapies to surgery are mandatory for combating the disease. These adjuvant therapies include radiotherapy and chemotherapy. More than 80% of the chemotherapeutics used today to combat cancers are pro-apoptotic agents, while numerous cancer types are naturally resistant to apoptosis such as gliomas,[2] melanomas,[3] pancreas cancers,[4] NSCLCs,[5] and esophageal cancers,[6] and for diverse reasons metastatic cancers.[7,8] It is therefore mandatory to identify novel therapeutics aiming to kill cancer cells resistant to apoptosis. Natural products remain a precious and largely unexplored reservoir from which to identify novel anti-cancer compounds.[9]

The cosmopolitan bright-red alga *Sphaerococcus coronopifolius*, Stackhouse 1797 (family Sphaerococcaceae), generally growing on rocks in shallow areas, has yielded a number of interesting brominated diterpenes of diverse molecular architectures.[10,11]

In the course of our ongoing investigations aiming at the isolation of bioactive metabolites from marine organisms of the Greek seas,[12,13] we studied the chemical composition of the red alga *S. coronopifolius*, collected from the West coast of Corfu island. In this report, we describe the isolation, and structure elucidation of coronone (**1**) featuring an unprecedented skeleton, possessing the gross tricyclic ring system of norsphaerol,[14] the new neodolastane diterpene alcohol sphaerostanol (**2**), and the new dicyclic derivative 10*R*-hydroxy-bromocorodienol (**3**), from the organic extract of *S. coronopifolius*, along with the isolation of 13 previously reported (**4**–**16**) terpenes. The molecular structures of the new natural products were established by 1D and 2D NMR, IR, UV, and high-resolution mass spectral measurements, and the absolute stereochemistry of metabolite **3** was determined using the modified Mosher's method.[15]

All compounds were evaluated for their in vitro growth inhibitory effect against four human apoptosis-resistant (U373, A549, SKMEL-28, OE21) and two human apoptosis-sensitive (PC-3, LoVo) cancer cell lines; they were found to possess significant, but variable antitumor activity.

* Corresponding author. Tel./fax: +30 210 7274592.
E-mail address: roussis@pharm.uoa.gr (V. Roussis).

0968-0896/$ - see front matter © 2009 Elsevier Ltd. All rights reserved.
doi:10.1016/j.bmc.2009.12.025

Table 1
^{1}H NMR data[a] and NOESY correlations of compounds **1**–**3**

No.	**1**			**2**					**3**		
	^{1}H (δ)	m (J)	NOESY	^{1}H (δ)	m (J)	^{1}H (δ)[b]	m (J)	NOESY	^{1}H (δ)	m (J)	NOESY
1	β 1.73	m	11, 13	β 1.65	m	1.58	m	2β	α 2.22	m	13
	α 1.10	m	11, 12	α 1.21	m	0.97	m	13, 17	β 1.77	m	14
2	β 1.86	ddd 14.6, 9.1, 5.6	3, 20	β 1.91	m	1.73	dtd 13.3, 9.6, 7.0	1β, 3, 19	α 1.82	m	13
	α 1.21	m	17, 20	α 1.37	m	1.19	m	19	β 1.69	m	
3	1.12	m	2β, 5β, 13	1.14	q 9.1	0.94	m	2β, 14	1.71	m	17a
4	—	—	—	—	—	—	—	—	—	—	—
5	α 1.71	m	6α, 6β, 17, 19	α 1.75	dd 14.5, 7.0	1.56	m	6β, 17, 20	α 1.93	dt 16.6, 4.6	6α, 13, 16
	β 1.36	m	3, 8, 13	β 1.24	m	0.97	m	6β, 8, 12, 14	β 1.77	m	6α, 17b
6	β 1.91	m	5α, 8, 16	β 2.05	dd 16.2, 7.0	2.17	ddd 16.2, 7.9, 1.2	5α, 5β, 8	α 2.26	m	5α, 5β
	α 1.41	m	5α, 12, 16, 17	α 1.35	m	1.28	m	13, 17	β 1.18	dt 14.1, 4.6	8, 17b
7	—	—	—	—	—	—	—	—	—	—	—
8	4.98	dd 13.2, 4.4	5β, 6β, 9β, 13	4.03	dd 12.4, 3.7	3.85	dd 12.4, 3.8	5β, 6β, 9β, 10β, 12	3.88	dd 12.4, 4.6	6β, 9β, 10, 12
9	α 2.59	ddd 14.3, 13.2,	10, 16	α 2.44	tdd 13.2, 12.4,	2.60	tdd 13.7, 12.4,	10α, 16	α 2.41	td 12.4, 11.6	16
	β 2.25	3.2	8, 10	β 2.02	4.2	1.98	4.2	8	β 2.35	dt 12.4, 4.6	8, 10
		dm 14.3			ddt 13.2, 4.6, 3.7		ddt 13.7, 4.6, 3.8				
10	4.43	br s	9α, 9β, 11	α 1.71	m	1.51	m	9α, 15	3.26	br dd 11.6,	8, 9β, 12, 15
				β 1.52	m	1.16	m	8, 15		4.6	
11	2.63	br s	1α, 1β, 10, 12, 13	—	—	—	—	—	—	—	—
12	2.30	br d 12.6	1α, 6α, 11, 16, 17	1.56	d 5.8	1.26	m	5β, 8, 15	1.44	d 9.1	8, 10, 14
13	2.11	dt 7.3, 12.6	1β, 3, 5β, 8, 11	3.92	ddd 9.5, 5.8, 2.9	3.58	ddd 9.5, 5.8, 2.9	1α, 6α, 16, 17	5.52	dd 15.8, 9.1	1α, 2α, 5α, 16
14	—	—	—	1.68	m	1.45	m	3, 5β	5.60	dt 15.8, 6.2	1β, 12
15	2.18	s	16	1.46	s	1.43	s	10α, 10β, 12	1.06	s	10
16	0.87	s	6α, 6β, 9α, 12, 15	1.32	s	1.51	s	9α	1.18	s	5α, 9α, 13
17	0.74	s	5α, 6α, 12	0.73	s	0.50	s	1α, 5α, 6α, 13, 18	a 4.81	t 2.1	3
									b 4.72	dd 2.1, 1.6	5β, 6β
18	1.51	m	19, 20	1.53	m	1.39	m	17	1.41	br hept 6.6	
19	0.92	d 6.4	5α, 18	0.83	d 6.6	0.85	d 6.6	2α, 2β	0.83	d 6.6	
20	0.83	d 6.4	2α, 2β, 18	0.92	d 6.6	0.90	d 6.6	5α	0.75	d 6.6	
11OH				2.67	br s						
13OH				1.84	d 2.9						

[a] ^{1}H (400 MHz) recorded in $CDCl_3$ (δ_H 7.24), chemical shifts are expressed in ppm and J values in Hz.
[b] ^{1}H (400 MHz) recorded in C_6D_6 (δ_H 7.16).

Table 2
^{13}C NMR data[a] and HMBC (^{13}C→^{1}H) correlations of compounds **1**–**3**

No.	**1**			**2**			**3**		
	^{13}C (δ)	Type[b]	HMBC	^{13}C (δ)	Type[b]	HMBC	^{13}C (δ)	Type[b]	HMBC
1	26.1	CH_2	2β	22.3	CH_2		27.7	CH_2	3, 13, 14
2	27.7	CH_2	1β, 3	28.0	CH_2	3	31.7	CH_2	1α, 3
3	58.5	CH	2α, 17, 19, 20	56.6	CH	17, 19, 20	55.3	CH	2β, 5α, 17a, 17b, 19, 20
4	43.3	C	3, 5α, 6β, 17	44.7	C	3, 5α, 6α, 6β, 14, 17	153.8	C	2α, 2β, 5α, 17a, 17b
5	34.9	CH_2	3, 6α, 17	33.7	CH_2	6α, 6β, 17	25.3	CH_2	3, 17a, 17b
6	35.0	CH_2	16	35.5	CH_2	16	39.1	CH_2	8, 12, 16
7	39.9	C	5α, 11, 12, 16	41.0	C	5α, 6β, 16	44.7	C	5α, 9α, 9β, 12, 16
8	55.9	CH	6α, 9α, 10, 12, 16	69.0	CH	9β, 16	63.8	CH	6α, 9α, 9β, 12, 16
9	39.6	CH_2		31.1	CH_2		39.1	CH_2	
10	68.3	CH	9α, 11, 12	42.9	CH_2	15, 11-OH	74.5	CH	9α, 9β, 15
11	55.0	CH	9β	73.0	C	9α, 10β, 15	73.5	C	15
12	44.9	CH	6β, 10, 11, 13, 16	58.9	CH	14, 15, 16	59.3	CH	6α, 13, 14, 15, 16
13	49.1	CH	1β, 11, 12, 17	71.2	CH	12, 14	125.3	CH	1α, 12
14	210.5	C	11, 15	63.0	CH	5α, 12, 17	134.8	CH	1α, 2α, 12, 13
15	28.0	CH_3		33.4	CH_3		26.2	CH_3	
16	23.5	CH_3	8, 12	20.3	CH_3	12	14.3	CH_3	8, 12
17	10.9	CH_3	3, 5β, 13	14.0	CH_3	3, 14	112.4	CH_2	3, 5α
18	31.0	CH	2α, 3, 19, 20	30.7	CH	3, 19, 20	29.8	CH	19, 20
19	22.4	CH_3	3, 20	23.0	CH_3	20	20.5	CH_3	20
20	23.0	CH_3	3, 19	23.3	CH_3	19	21.6	CH_3	19

[a] ^{13}C (50.3 MHz) recorded in $CDCl_3$ (δ_C 77.0), chemical shifts are expressed in ppm.
[b] Multiplicities inferred from DEPT and HMQC experiments.

2. Results and discussion

2.1. Chemistry

S. coronopifolius seaweeds were collected in Palaiokastritsa bay on the West side of Corfu island and the CH_2Cl_2/MeOH extract of the freeze-dried alga was subjected to a series of gravity column chromatography fractionations on silica gel using mixtures of cyclohexane/EtOAc as mobile phase, as well as reverse and normal phase high performance liquid chromatography (HPLC) separations, using CH_3CN, and mixtures of cyclohexane with EtOAc or CH_3Cl as eluent, to yield compounds **1**–**3** in pure form.

Metabolite **1** was obtained as colorless viscous oil. The molecular formula $C_{20}H_{33}BrO_2$, which was derived from HRMS and NMR data (Tables 1 and 2), requires four degrees of unsaturation. The LRCI-MS isotope clusters at *m/z* 367:369 $[(M+H)–H_2O]^+$ (ratio 1.0:0.9), at *m/z* 323:325 $[(M+H)–H_2O–CH_3CHO]^+$ (ratio 1.0:1.0), and at *m/z* 287 $[M–H_2O–HBr]^+$ indicated the presence of a bromine atom, an acetyl, and a hydroxyl group. This was supported by the IR spectrum which contained an intense band at 1692 cm^{-1} (C=O stretch), and showed the presence of hydroxyl functionality (ν_{max} 3440 cm^{-1}). Analysis of the NMR data revealed the presence of an acetyl group (δ_H 2.18 s; δ_C 210.5 s, 28.0 q), a bromomethine (δ_H 4.98 dd; δ_C 55.9 d), and an oxygenated methine (δ_H 4.43 br s; δ_C 68.3 d). Interpretation of the ^1H–^1H COSY, HSQC, and HMBC data allowed the remaining three degrees of unsaturation to be assigned to a tricyclic carbon skeleton. Partial structures from C-5 to C-6 (A), C-8 to C-10 (B), also present in other previously reported metabolites of *S. coronopifolius*, and substructure C were clearly revealed by extensive analyses of the ^1H NMR, COSY, and HSQC spectra of **1** (Fig. 1). Complementary HMBC correlations (Table 2) allowed us to confirm the structure of these fragments. Detailed analyses of the proton and carbon chemical shifts and of the correlations observed in the HMBC spectra, confidently established the gross structure shown for **1** (Fig. 1), by connecting segments A, B, and C. In particular, the long range heteronuclear couplings observed in the HMBC spectrum, from H_3-17 to C-3, C-4, C-5, and C-13, from carbon C-4 to protons H-3, H-5α, and H-6β and from the latter to C-12 showed that units A and C were connected through the quaternary carbon C-4. The acetyl bearing carbon C-11 had to be linked to C-10, as depicted from the correlations of proton H-11 with C-10 and C-14, as well as of C-11 with H-9β,

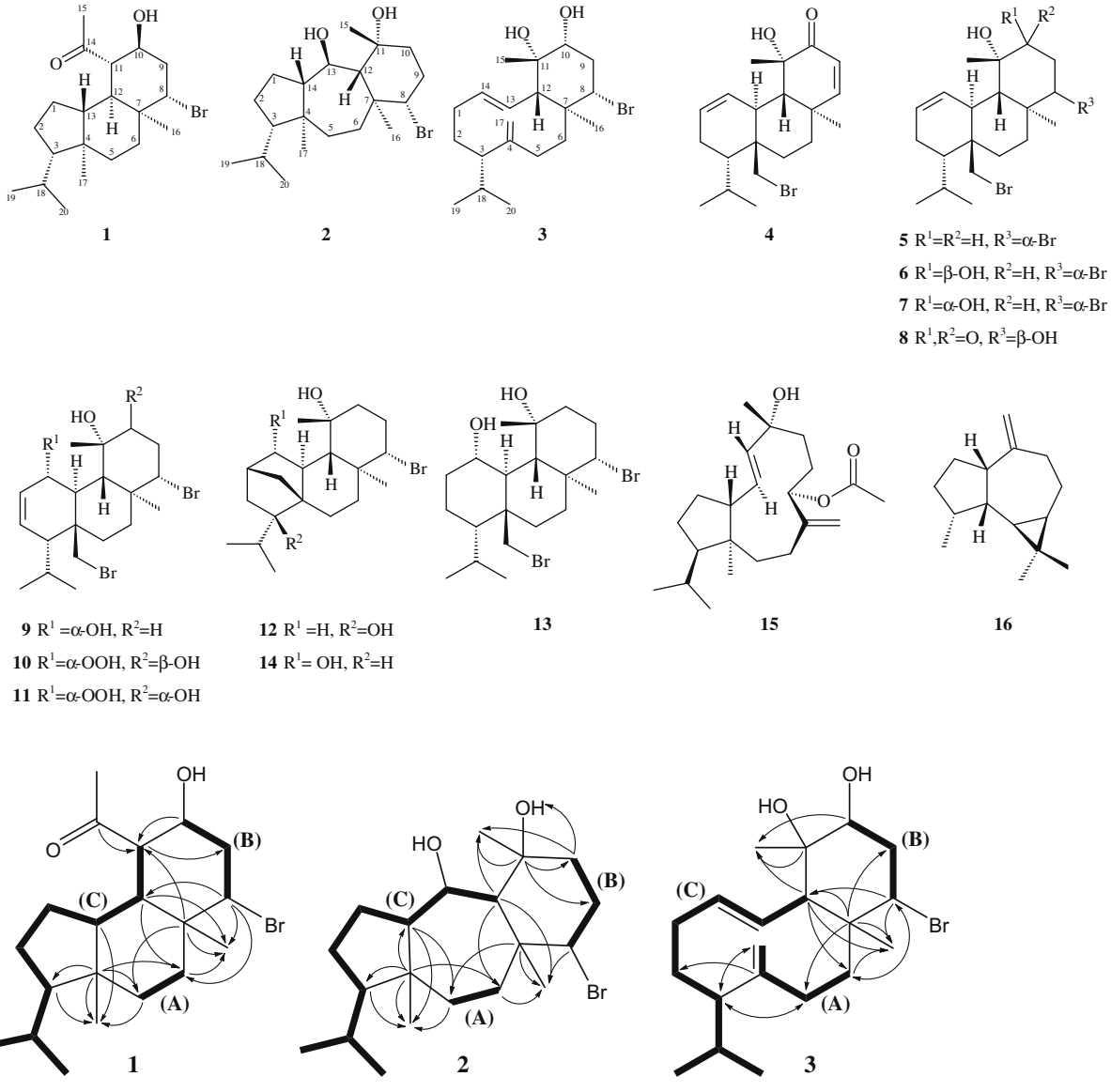

Figure 1. Partial structures of **1**, **2**, and **3**. ▬ COSY and HSQC correlations, → key C→H HMBC correlations.

although no COSY correlation was observed between the broad singlet protons H-10 and H-11. The connection of the partial structures through the fully substituted carbon C-7 was determined from the HMBC cross peaks of C-6, C-7, C-8, and C-12 with methyl H_3-16, as well as from the correlations of C-7 with H-5α and H-11, and of C-8 with both H-6α and H-12.

The relative configurations for the eight stereocenters of the tricyclic framework were assigned primarily on the basis of the ^{1}H NMR coupling constants and NOESY experiments. NOE correlations between H-3, H-5β, and H-13, and of the latter with H-1β, as well as correlations between H-1α, H-12, and H_3-17 required trans ring fusion and indicated that protons H-1β, H-3, H-5β, and H-13 had the same β-configuration, while H-1α, H-12, and methyl H_3-17 had the opposite. The NOESY spectrum showed prominent NOE interactions of proton H-8 with H-13 and of H_3-16 with H-12 suggesting an unusual cis-fusion of the six-membered rings. Methyl H_3-16 was positioned co-facial to proton H-12, based on the NOE correlations of both H_3-16 and H_3-17 with H-6α and H-12. The stereochemistry at C-8 was deduced by NOE correlations between proton H-8 and H-5β, H-6β, H-9β and H-13, methyl H_3-16 with H-6α and H-9α, and H_3-17 with H-5α and H-6α. Moreover, the couplings observed in the NOESY spectrum from H-10 to both H_2-9 and H-11, and from H-11 to both H_2-1, to H-12 and H-13, secured the relative stereochemistry at chiral centers C-10 and C-11, thereby defining the structure of metabolite **1** which was named coronone (Fig. 2).

In an attempt to determine the absolute stereochemistry of coronone (**1**) using the modified Mosher's method[15] **1** was treated with (*R*)- and (*S*)-MTPA chloride. Analysis of the reaction product revealed that, the secondary hydroxyl was not esterified as expected but was eliminated leading to formation of the $\Delta^{10,11}$-trisubstituted double bond. The structure of the 10-deoxy-analogue of coronone (**1**) was determined on the basis of its ^{1}H, HSQC, and COSY NMR spectra.

The structural characterization of metabolite **2** was carried out in an analogous manner. Sphaerostanol (**2**) was isolated as colorless oil, possessing the molecular formula $C_{20}H_{35}BrO_2$, established from the high-resolution mass measurement that required three unsaturation equivalents. The hydroxyl group functionalities were supported by both IR spectrum (ν_{max} 3368 cm^{-1}), and the positive LRCI-MS measurements that showed ions at *m/z* 369:371 $[(M+H)–H_2O]^+$ (ratio 1.0:0.7), at *m/z* 351:353 $[(M+H)–2H_2O]^+$ (ratio 1.0:0.9), at *m/z* 289 $[(M+H)–H_2O–HBr]^+$, and at *m/z* 271 $[(M+H)–2H_2O–HBr]^+$, also indicating the presence of a bromine atom. ^{1}H and ^{13}C NMR data ($CDCl_3$) of **2** (Tables 1 and 2) confirmed the above mentioned, by exhibiting signals for a bromomethine ($\delta_{H,C}$ 4.03 dd, 69.0 d), an oxygenated methine ($\delta_{H,C}$ 3.92 ddd, 71.2 d), an oxygenated quaternary carbon (δ_C 73.0 s), and two exchangeable hydroxyl protons (δ_H 1.84 br s and 2.67 d). Due to the proximity of diagnostic signals (H-1β, H-12, and H-14) when the ^{1}H NMR spectrum was measured in $CDCl_3$, the ^{1}H NMR, COSY, NOESY, and HSQC experiments were also recorded in C_6D_6. Analyses of the COSY, HSQC, and HMBC spectra resulted in the unambiguous assignment of all protons and carbons to a neodolastane skeleton. The NMR data of **2** showed close similarities with that of **1** suggesting similar partial structures A, B, and the isopropyl-cyclopentane part of substructure C (Fig. 1). Cross peaks in the COSY spectrum revealed couplings between H-13 and H-12, 13-OH, and H-14, and from there to both H-1α and H-1β. Moreover, the heteronuclear long range couplings of carbon C-13 with H-12 and H-14, and of C-12 with hydroxyl proton 13-OH confidently established the position of the oxygenated methine in substructure C. Additional HMBC correlations joined segments A, B, and C through the quaternary carbons C-4, C-7, and C-11 (Table 2 and Fig. 1).

The relative stereochemistry of **2** was elucidated on the basis of the NOESY experiments (2D in $CDCl_3$ and 1D in C_6D_6). The NOE correlations observed (Table 1 and Fig. 3), between H-3/H-14, H-14/H-5β, H-1α/H-13, H-1α/H_3-17, H-13/H_3-17, H_3-17/H-18, and H-8/H-5β, H-8/H-6β, H-5β/H-12, H-6α/H-13, and H-13/H_3-16 secured the all-trans conformation of the molecule by establishing the stereochemistry at C-3, C-4, C-7, C-8, C-12, C-13, and C-14. Additionally, H-l0α, H-10β, and H-12 exhibited positive NOE responses upon irradiation of H_3-15, thus confirming the β-equatorial configuration of H_3-15, in metabolite **2**, named sphaerostanol.

Compound **3** was isolated as colorless oil. Both ^{13}C NMR data and HR-FAB-MS measurements supported the molecular formula $C_{20}H_{33}BrO_2$. All spectroscopic data, including 1D and 2D NMR, IR, UV, and MS measurements showed close similarity with those of bromocorodienol (**17**),[16] suggesting that it was its 10-hydroxy derivative. All protonated carbons and their protons were assigned by the COSY and HSQC experiments and the structure elucidation was assisted by analyses of the HMBC experiments (Fig. 1). Both COSY correlations between H-10 and methylene protons H_2-9, and HMBC correlations from C-10 to H_2-9 and H_3-15, clearly positioned the secondary hydroxyl group at C-10.

The relative stereochemistry shown for **3** (Fig. 4) was assigned by interpretation of ^{1}H NMR coupling constants and NOESY data. The H-10 signal showed NOE correlations to the signals of H-8, H-9β, H-12, and H_3-15, thereby establishing the relative stereochemistry at C-10, and the structure of metabolite **3** as 10R^*-hydroxy-bromocorodienol.

The absolute stereochemistry of **3** was determined by application of the modified Mosher's method.[15] When **3** was treated with

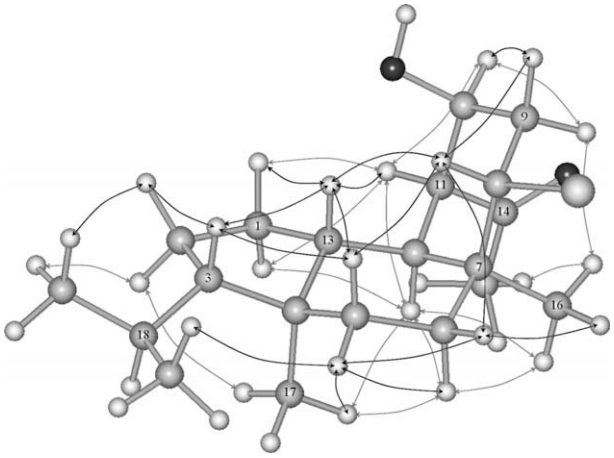

Figure 2. Relative configuration and NOE correlations for metabolite **1**.

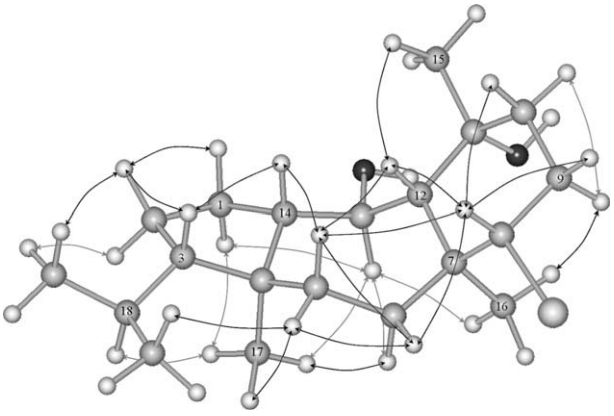

Figure 3. Relative configuration and NOE correlations for metabolite **2**.

(*R*)- and (*S*)-MTPA chloride, the secondary hydroxy group at C-10 reacted to give the (*S*)- and (*R*)-MTPA derivatives, respectively. The ^{1}H NMR chemical shifts of the MTPA derivatives of **3** were assigned by analysis of ^{1}H, HSQC, and COSY NMR spectra. The calculation of the $\Delta\delta_{S-R}$ values, shown in Figure 5, defined the absolute stereochemistry of C-10 as *R* and subsequently, on the basis of its relative configuration, established the absolute stereochemistry of **3** as depicted.

Compounds **4**–**16** were identified by comparison of their spectroscopic and physical characteristics with those reported in the literature as sphaerococcenol A (**4**),[11,17–19] bromosphaerol (**5**),[17,19–21] 12*S*-hydroxy-bromosphaerol (**6**),[17,22] 12*R*-hydroxy-bromosphaerol (**7**),[17,23] 14*R*-hydroxy-13,14-dihydro-sphaerococcenol A (**8**),[17] bromosphaerodiol (**9**),[17,24] 1*S*-hydroperoxy-12*S*-hydroxy-bromosphaerol-B (**10**),[17,23] 1*S*-hydroperoxy-12*R*-hydroxy-bromosphaerol-B (**11**),[17] 4*R*-hydroxy-1-deoxy-bromotetrasphaerol (**12**),[25] 1*S*-hydroxy-1,2-dihydro-bromosphaerol (**13**),[26,27] bromotetrasphaerol (**14**),[28] sphaerollane I (**15**),[10] and (−)allo-aromadendrene (**16**).[19]

The co-occurrence of compounds **1**, **2**, and **3** in the same organism indicates the possibility of a common biosynthetic origin from the same rearranged carbocation, resulting from genanyl-geranyl-pyrophosphate, as previously proposed for **17**,[16] that could be formulated by the biogenetic pathway depicted in Scheme 1. Thus, nucleophilic substitution of a H_2O molecule and bromonium ion-induced cyclization can produce the cycloheptane-ring that undergoes a ring contraction to yield the methyl ketone, and finally metabolite **1** after addition of a H_2O molecule. Successive additions of H_2O molecules with a parallel bromonium ion evolved cyclization can produce sphaerostanol (**2**). Alternatively, **3** could be originated by addition of H_2O, from bromocorodienol (**17**).[16]

Diterpenes of the neodolastane class have previously been isolated only from fungi species,[29–32] while diterpenes of the bromocorodienol skeleton have been isolated, only from the red alga *S. coronopifolius*.

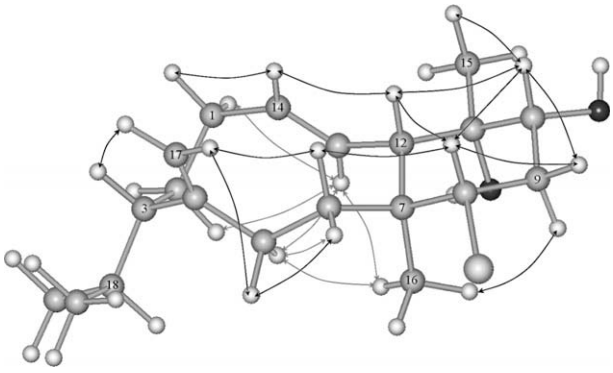

Figure 4. Relative configuration and NOE correlations for metabolite **3**.

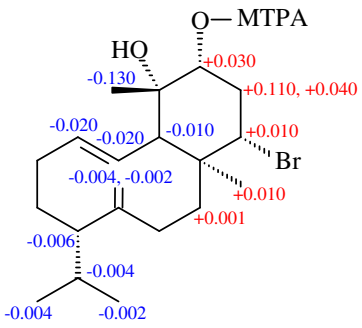

Figure 5. $\Delta\delta_{S-R}$ values (ppm) for the C-10 MTPA derivatives of **3** in $CDCl_3$.

2.2. Pharmacological evaluation

The in vitro antitumor activity of compounds **1**–**16** have been determined in four human apoptosis-resistant and two human apoptosis-sensitive cancer cell lines. The four human apoptosis-resistant cancer cell lines include the U373 glioblastoma (GBM),[33,34] the A549 non-small-cell-lung cancer (NSCLC),[35] the SKMEL-28 melanoma cell line[36] and the OE21 esophageal cancer cell line.[37] The two apoptosis-sensitive cancer cell lines include the PC-3 prostate[38] and the LoVo colon[39] cancer cell lines. The IC_{50} in vitro growth inhibitory values of the metabolites were determined by means of the MTT colorimetric assay as detailed elsewhere.[33,40,41] The origin of the cell lines used in the current study and the culture media are also fully detailed in Refs. 33, 40, and 41. We report in Table 3 the mean IC_{50} in vitro growth inhibitory values (±SEM and ±SD) we obtained with respect to sextuplicates for each individual compound with respect to each individual cell line.

We first investigated as whether the various cell lines under study displayed distinct profiles of sensitivity to the 16 compounds listed in Table 3 in relation to apoptosis sensitivity versus resistance. The data illustrated in Figure 6A show that all six cancer cell lines roughly displayed similar sensitivity to the 16 compounds. These data therefore strongly suggest that the compounds under study are able to overcome the natural resistance of certain cancer cell types to apoptosis.

The data in Figure 6B represent the mean IC_{50} values ± SEM calculated on the six human cancer cell lines for the 16 compounds under study (Table 3). Actual variability appears between the 16 compounds under study in term of antitumor activity. We thus investigated as whether a SAR could be evidenced for the 16 compounds under study according to the fact that about one log in difference of activity has been observed between the less (**2**, **12**, **16**) and the most (**4**, **6**, **8**) potent compounds (Fig. 6B). It appears that compounds featuring the sphaerane carbon skeleton (**4**–**11**, **13**) exhibit increased antitumor activity. Among them the more potent agents (**4**, **6**, **8**) comprise a $\Delta^{1,14}$ double bond and a carbonyl or hydroxyl group at carbon C-10. The stereochemistry of the hydroxyl bearing carbon C-10 seems to affect the activity, with β-oriented hydroxyl derivatives being more active (**6**, **10** and **7**, **11**, respectively). Furthermore, bromotetrasphaerol (**14**) exhibited activities which were two-times stronger than those of 3-α-hydroxy-derivative (**12**). It is clear that slight structural alterations on the diterpene skeleton cause significant variations in their antitumor activity making these preliminary results a stimulus for further structure–activity investigations.

Lastly, we made use of computer-assisted phase-contrast microscopy (quantitative videomicroscopy)[42,43] to grossly decipher the mechanisms of action of the three most active compounds under study, that is, **4**, **6**, and **8**, on the apoptosis-resistant U373 glioblastoma cell line. This original approach already enabled us for example to identify cytotoxic effects including pro-autophagic-related cell death induced by sodium pump inhibitors in U373 GBM cells[34] and lysosomal membrane permeabilization-related cell death in A549 NSCLC cells[35] as well as cytostatic effects in glioma[33] and prostate cancer[40] cells. The morphological information revealed by Figures 7A–C thus clearly indicate that compounds **4**, **6**, and **8** exert their growth inhibitory activity in vitro (as revealed by means of the MTT colorimetric assay; Table 3 and Fig. 6) through cytostatic and not cytotoxic processes, a feature that therefore explains, at least partly, why these compounds partially overcome the natural resistance of U373 glioblastoma cells to apoptosis. Additional subtle differences can be highlighted between the antitumor effects displayed by compounds **4**, **6**, and **8** when U373 GBM cells are analyzed at higher magnification thanks to the quantitative videomicroscopy approach. Indeed, compounds **4** and **6** are actual

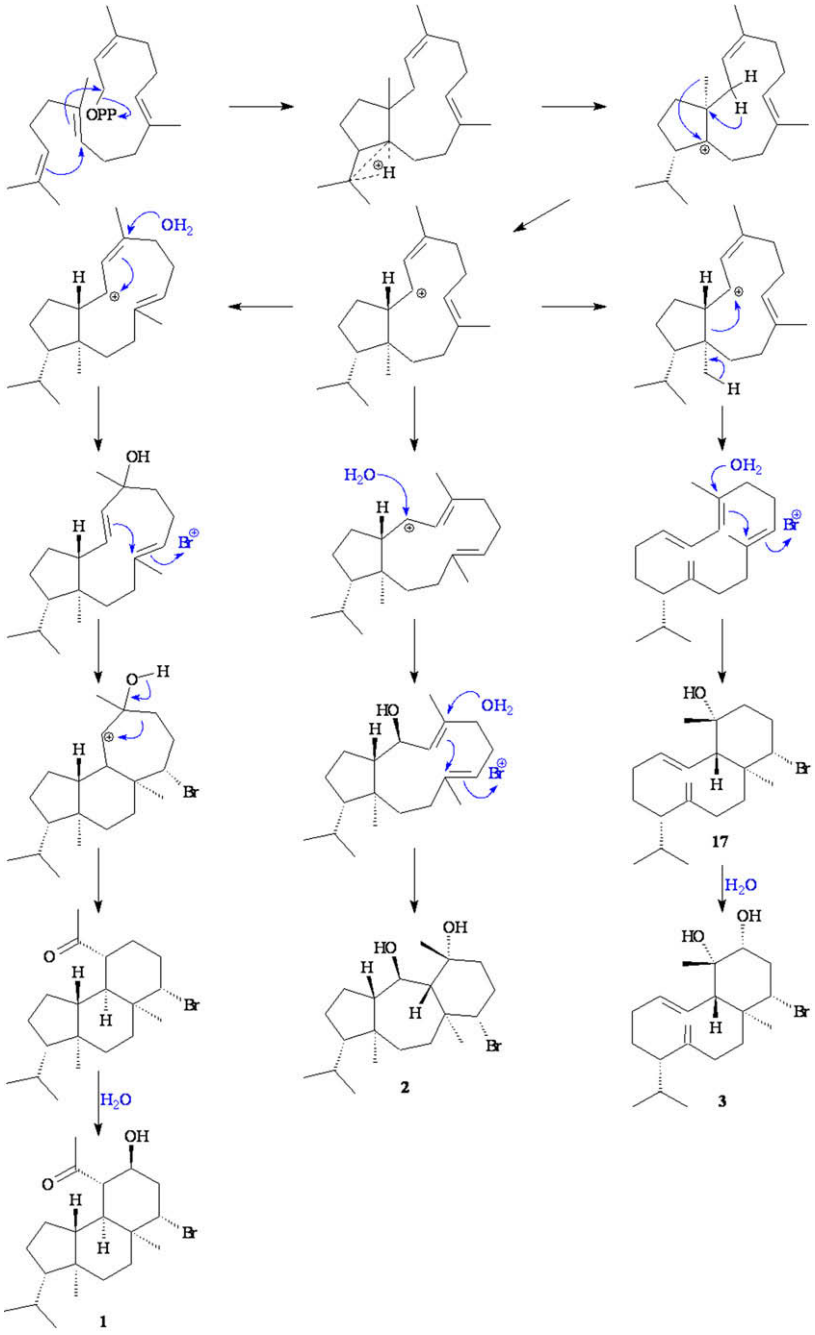

Scheme 1. Proposed biogenetic origin of metabolites **1**–**3**.

cytostatic compounds that delay U373 GBM cell growth through marked decreases in mitosis entry for compound **4** (Fig. 7A) and marked increases in mitosis length for compound **6** (from an average duration of 2–3 h in control condition (Fig. 7B) to >15 h in experimental conditions in which U373 GBM cells are treated for 3 days with 16 μM of **6** (Fig. 7B). In contrast, compound **8** displays cytostatic effects through indirect effects: it does not increase mitosis length but it induces marked vacuolization processes that delay cell proliferation (Fig. 7C). This vacuolization processes can relate to either pro-autophagic[34] or to the induction of lysosomal membrane permeabilization-related cell death[35] as we already evidenced previously with other types of natural compounds from terrestrial origin. One marine compound, Kahalalide F (isolated from *Bryopsis* sp.), alters the function of the lysosomal membrane and induces cancer cell necrosis in vivo (oncosis), with selectivity between cancer and normal cells and an activity in cancer cells that is independent of multidrug resistance (MDR) expression in cancer cells.[44–47] Further biochemical and molecular biology-related experiments are warranted to precisely decipher the mechanisms of action by which the more active compounds under study exert their antitumor activity, with the possibility that such compounds display unique mechanisms of action as does Kahalalide F, which is currently undergoing Phase II clinical trials.

3. Experimental

3.1. General experimental procedures

Optical rotations were measured on a Perkin–Elmer model 341 polarimeter with a 10-cm cell. UV spectra were acquired in

Table 3
IC_{50} in vitro growth inhibitory values of compounds **1–16**

Compounds	IC_{50} in vitro growth inhibitory concentrations (μM)						Mean ± SEM (±SD)
	U373	A549	OE21	SKMEL-28	PC-3	LoVo	
1	31 ± 1 (±3)	42 ± 2 (±5)	30 ± 2 (±6)	38 ± 1 (±3)	30 ± 2 (±6)	28 ± 1 (±2)	32 ± 2 (±5)
2	85 ± 4 (±10)	97 ± 6 (±14)	60 ± 3 (±6)	96 ± 6 (±13)	74 ± 2 (±6)	64 ± 3 (±9)	76 ± 6 (±16)
3	60 ± 2 (±5)	64 ± 1 (±3)	33 ± 2 (±5)	62 ± 1 (±3)	48 ± 2 (±4)	24 ± 3 (±7)	46 ± 7 (±17)
4	3.2 ± 0.1 (±0.2)	3.7 ± 0.1 (±0.2)	3.0 ± 0.1 (±0.2)	5.2 ± 0.3 (±0.7)	3.7 ± 0.1 (±0.3)	2.8 ± 0.1 (±0.2)	3.3 ± 0.4 (±0.9)
5	30 ± 1 (±2)	35 ± 1 (±2)	28 ± 2 (±4)	34 ± 1 (±3)	30 ± 1 (±2)	23 ± 2 (±5)	29 ± 2 (±4)
6	16 ± 2 (±4)	19 ± 2 (±6)	19 ± 1 (±2.0)	22 ± 1 (±2)	12 ± 2 (±5)	9 ± 1 (±2)	16 ± 2 (±5)
7	25 ± 1 (±2)	28 ± 1 (±4)	25 ± 1 (±2)	29 ± 1 (±2)	26 ± 1 (±2)	26 ± 1 (±2)	27 ± 1 (±2)
8	7.2 ± 0.4 (±0.9)	18 ± 1 (±4)	8.4 ± 0.2 (±0.4)	21 ± 1 (±3)	8.1 ± 0.3 (±0.8)	5.3 ± 0.4 (±0.9)	11 ± 3 (±7)
9	22 ± 1 (±2)	24 ± 1 (±2)	15 ± 1 (±3)	31 ± 1 (±2.0)	26 ± 2 (±4)	20 ± 2 (±4)	23 ± 2 (±5)
10	22 ± 1 (±2)	26 ± 1 (±2)	27 ± 1 (±3)	28 ± 1 (±2)	28 ± 1 (±3)	28 ± 1 (±2)	26 ± 1 (±3)
11	32 ± 1 (±2)	40 ± 2 (±6)	25 ± 1 (±3)	31 ± 4 (±9)	30 ± 2 (±4)	22 ± 1 (±3)	30 ± 3 (±6)
12	75 ± 1 (±3)	63 ± 2 (±4)	64 ± 3 (±6)	>100	43 ± 3 (±7)	56 ± 3 (±6)	>43
13	25 ± 1 (±2)	28.6 ± 0.3 (±0.7)	20 ± 1 (±3)	26 ± 1 (±2)	25 ± 1 (±2)	23 ± 1 (±3)	25 ± 1 (±3)
14	34 ± 2 (±4)	38 ± 2 (±5)	33 ± 2 (±5)	43 ± 1 (±3)	30 ± 2 (±5)	26 ± 1 (±3)	34 ± 2 (±6)
15	20 ± 1 (±3)	44 ± 2 (±5)	34 ± 3 (±7)	57 ± 2 (±5)	34 ± 2 (±4)	23 ± 1 (±4)	35 ± 6 (±14)
16	71 ± 2 (±6)	79 ± 2 (±6)	83 ± 3 (±8)	>100	35 ± 2 (±4)	63 ± 2 (±6)	>35

The values obtained by means of the MTT colorimetric assay in six distinct human cancer cell lines, which include a glioblastoma (U373), a non-small-cell-lung cancer (A549), an esophageal cancer (OE21), a melanoma (SKMEL-28), a prostate cancer (PC-3) and a colon cancer (LoVo) models. The cancer cells have been cultured during three days in presence of the compounds and the data are reported as mean IC_{50} ± SEM (±SD) values calculated on sextuplicates for each compound and for each cell line.

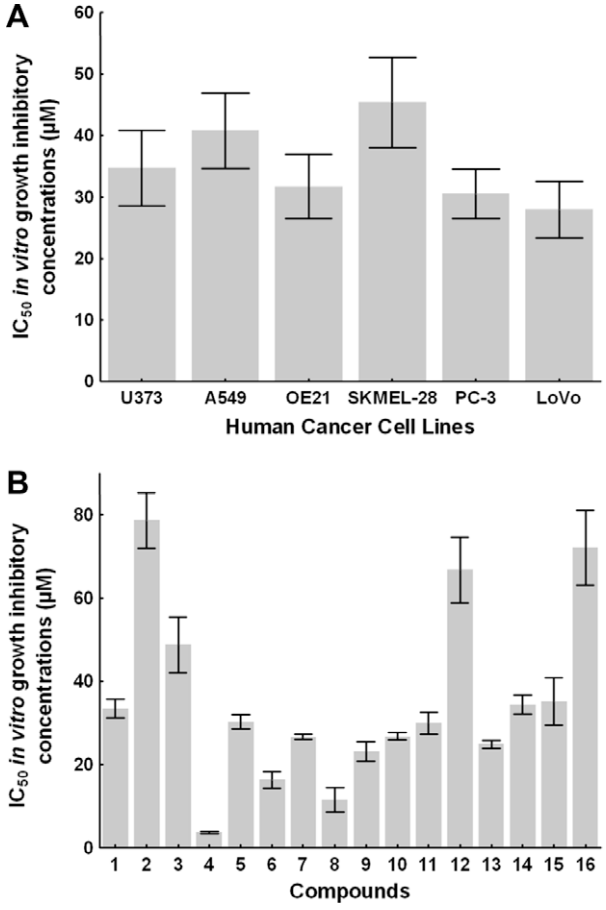

Figure 6. (A) Mean ± SEM values of the 16 IC_{50} values reported in Table 3 with respect to each cancer cell line on which the 16 compounds have been assayed by means of the MTT colorimetric test. (B) Mean ± SEM values of the 6 IC_{50} values reported in Table 3 with respect to each compound that has been assayed on six distinct human cancer cell lines by means of the MTT colorimetric test.

spectroscopic grade $CHCl_3$ on a Shimadzu UV-160A spectrophotometer. IR spectra were obtained using a Paragon 500 Perkin–Elmer spectrophotometer. NMR spectra were recorded using a Bruker AC 200 and Bruker DRX 400 spectrometers. Chemical shifts are given on a δ (ppm) scale using TMS as internal standard. The NMR experiments (COSY, HSQC, HMBC, 1D and 2D NOESY) were performed using standard Bruker microprograms. The structures in Figures 2–4 were generated and optimized (energy: 44.97, 59.61, and 38.77 kcal/mol, respectively) by 'HyperChem™ 7.0' molecular modeling and simulation software (force field: MM+; optimization algorithm: Polak-Ribiere). High-resolution mass spectral data were provided by the University of Notre Dame, Department of Chemistry and Biochemistry, Indiana, USA. Low-resolution chemical ionization MS data were recorded on a Thermo DSQ Mass Detector using Direct Exposure Probe (DEP) and methane as the CI gas. Vacuum liquid chromatography (VLC) separation was performed with Kieselgel 60 (Merck), gravity column chromatography (GCC) was performed with Kieselgel 60H (Merck), thin-layer chromatography (TLC) was performed with Kieselgel 60 F_{254} aluminum support plates (Merck) and spots were detected after spraying with 15% H_2SO_4 in MeOH reagent and charring. HPLC separations were conducted using an Agilent 1100 model equipped with refractive index detector and a Kromasil 100 C18 5u (250 × 8 mm) or a SupelcoSil 5u (250 × 10 mm) HPLC column.

3.2. Plant material

S. coronopifolius was collected by SCUBA diving in Palaiokastritsa bay at the West coast of Corfu island, Greece, at a depth of 10–15 m in May of 2002. A specimen is kept at the Herbarium of the Laboratory of Pharmacognosy and Chemistry of Natural Products, University of Athens (ATPH/MO/201).

3.3. Extraction and isolation

S. coronopifolius was initially freeze-dried (291.4 g dry weight) and then exhaustively extracted with mixtures of CH_2Cl_2–MeOH (3/1) at room temperature. The combined extracts were concentrated to give a dark green residue (8.20 g), which was later subjected to vacuum liquid chromatography on silica gel, using a 10% step gradient of cyclohexane–EtOAc elution sequence. Fraction F3 (644.7 mg), eluted with 50% EtOAc in cyclohexane, was fractionated by gravity column chromatography, using a 5% step gradient of cyclohexane–EtOAc. Fraction F3.10 (24.8 mg), eluted with 25% EtOAc in cyclohexane, was further separated by normal phase HPLC using 18% EtOAc in cyclohexane as the mobile phase. Compounds **1** (2.1 mg) and **2** (0.9 mg) were isolated by reverse

phase HPLC with MeCN as eluent, from peak F3.10.2 (retention time 11.4 min) (3.3 mg). The CH_3CN soluble portion (306.7 mg) of fraction F4 (60% EtOAc in cyclohexane) (337.8 mg) was subjected to reverse phase HPLC, using CH_3CN as mobile phase. Peak F4.12 (retention time 12.6 min) (36.6 mg) was further fractionated by reverse phase HPLC with 100% MeCN. A final normal HPLC purification of peak P4.12.6 (retention time 25.4 min) (5.8 mg) with 45% cyclohexane in $CHCl_3$ yielded pure compound **3** (4.1 mg).

3.3.1. Coronone (1)

Colorless oil; $[\alpha]_D^{20}$ −54.5 (*c* 1.8, $CHCl_3$); UV $\lambda_{max}^{CHCl_3}$ nm (log ε): 245 (1.95), 273 (1.70); IR ($CHCl_3$) ν_{max} cm^{-1} 3440 (OH), 1692 (C=O); NMR data ($CDCl_3$), see Tables 1 and 2; CIMS (CH_4, DEP), *m/z* (rel int.%): 384:386 $[M+H]^+$ (2:2), 367:369 $[(M+H)-H_2O]^+$ (12:11), 323:325 $[(M+H)-H_2O-CH_3CHO]^+$ (2:2), 305 $[(M+H)-HBr]^+$ (97), 287 $[(M+H)-HBr-H_2O]^+$ (100), 269 (27), 245 (35), 203 (8), 149 (19), 107 (37), 81 (12); HR-FAB-MS *m/z* 385.1730 ($[M+H]^+$, calcd for $C_{20}H_{34}{}^{79}BrO_2$ 385.1742).

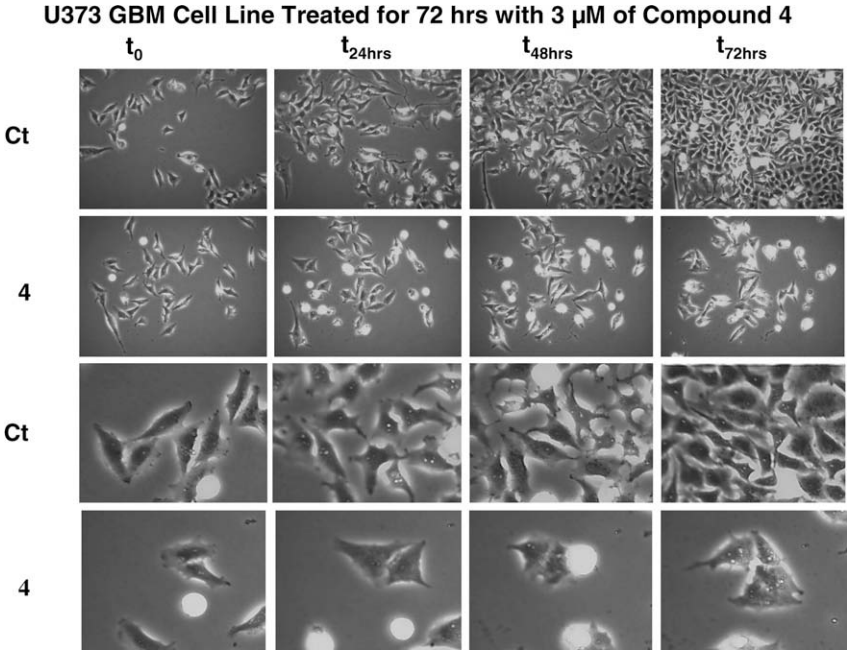

Figure 7A. Human U373 glioblastoma cells have been treated (or left untreated; control = Ct) for 72 h with 3 μM of compound **4** (a concentration that corresponds to its IC_{50} in vitro growth inhibitory concentration; see Table 3). These morphological illustrations indicate that compound **4** exerts its antitumor activity through cytostatic effects, which in turn occur through marked compound **4**-induced inhibition of cell entry into mitosis.

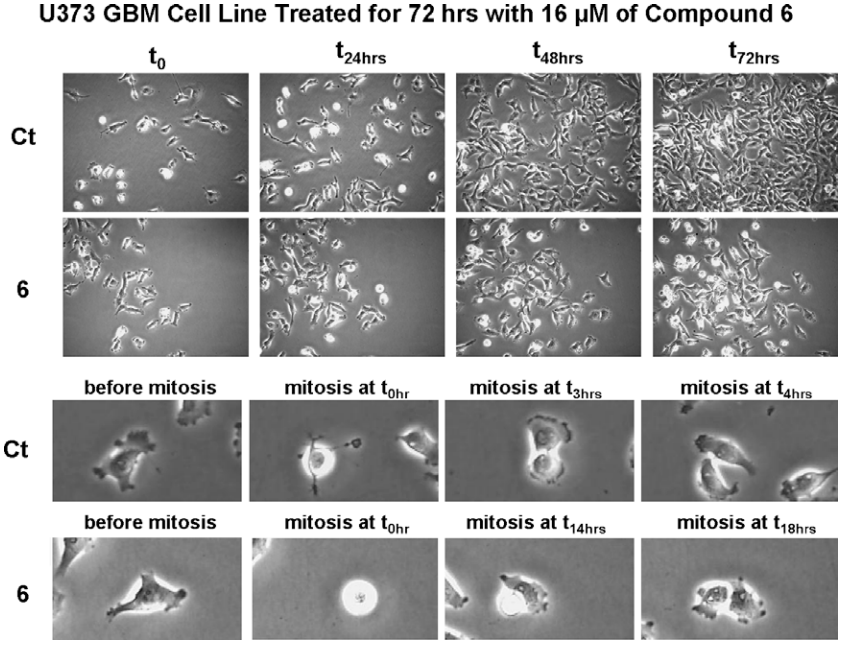

Figure 7B. Human U373 glioblastoma cells have been treated (or left untreated; control = Ct) for 72 h with 16 μM of compound **6** (a concentration that corresponds to its IC_{50} in vitro growth inhibitory concentration; see Table 3). These morphological illustrations indicate that compound **6** exerts its antitumor activity through cytostatic effects, which in turn occur through marked compound **6**-induced increases in mitosis duration.

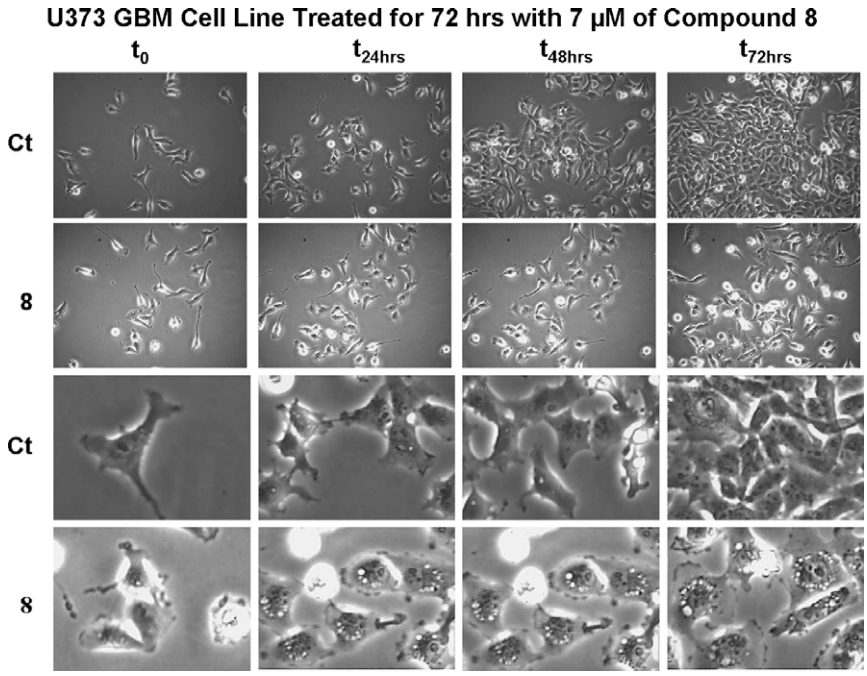

Figure 7C. Human U373 glioblastoma cells have been treated (or left untreated; control = Ct) for 72 h with 7 µM of compound **8** (a concentration that corresponds to its IC_{50} in vitro growth inhibitory concentration; see Table 3). These morphological illustrations indicate that compound **8** exerts its antitumor activity through cytostatic effects (see the lower magnifications at 48 and 72 h). These cytostatic effects seem to relate, at least partly, to autophagy and/or lysosomal membrane permeabilization processes as revealed by the marked vacuolization in the cytoplasm of compound **8**-treated U373 cells (see the higher magnifications).

3.3.2. Sphaerostanol (2)

Colorless oil; $[\alpha]_D^{20}$ +7.1 (*c* 1.5, $CHCl_3$); UV $\lambda_{max}^{CHCl_3}$ m (log ε): 735 (0.31); IR ($CHCl_3$) ν_{max} cm^{-1} 3368 (OH); NMR data ($CDCl_3$), see Tables 1 and 2; CIMS (CH_4, DEP), *m/z* (rel int.%): 369:371 $[(M+H)-H_2O]^+$ (4:3), 351:353 $[(M+H)-2H_2O]^+$ (9:8), 289 $[(M+H)-HBr-H_2O]^+$ (83), 271 $[(M+H)-HBr-2H_2O]^+$ (100), 255 (17), 227 (11), 173 (12), 149 (16), 109 (21), 107 (31), 81 (29); HR-FAB-MS *m/z* 369.1768 ($[M-OH]^+$, calcd for $C_{20}H_{34}{}^{79}BrO$ 369.1793).

3.3.3. 10*R*-Hydroxy-bromocorodienol (3)

Colorless oil; $[\alpha]_D^{20}$ +22.3 (*c* 4.6, $CHCl_3$); UV $\lambda_{max}^{CHCl_3}$ nm (log ε): 243 (2.10), 254 (1.95), 260 (1.80), 416 (1.08); IR ($CHCl_3$) ν_{max} cm^{-1} 3389 (OH), 3092 (=C—H), 886 (=CH); NMR data ($CDCl_3$), see Tables 1 and 2; CIMS (CH_4, DEP), *m/z* (rel int.%): 384:386 $[M+H]^+$ (4:4), 367:369 $[(M+H)-H_2O]^+$ (14:13), 349:351 $[(M+H)-2H_2O]^+$ (10:10), 312:314 (20:20), 305 $[(M+H)-HBr]^+$ (12), 287 $[(M+H)-HBr-H_2O]^+$ (100), 269 $[(M+H)-HBr-2H_2O]^+$ (59), 231 (16), 190 (14), 162 (15), 149 (14), 109 (17), 83 (38); HR-FAB-MS *m/z* 384.1660 ($[M]^+$, calcd for $C_{20}H_{33}{}^{79}BrO_2$ 384.1664).

Acknowledgments

This study was partially supported by the FP-39 EPAN program of the Greek Secretariat for Research and Technology and by the *Fonds Yvonne Boël* (Brussels, Belgium). R.K. is a research director with the *Fonds National de la Recherche Scientifique* (FNRS, Belgium).

References and notes

1. Boyle, P.; Levin, B. *World Cancer Report 2008*; World Health Organization, International Agency for Research on Cancer: Lyon, France, 2008.
2. Lefranc, F.; Brotchi, J.; Kiss, R. *J. Clin. Oncol.* **2005**, *23*, 2411.
3. Soengas, M. S.; Lowe, S. W. *Oncogene* **2003**, *22*, 3138.
4. El Maalouf, G.; Le Tourneau, C.; Batty, G. N.; Faivre, S.; Raymond, E. *Cancer Treat. Rev.* **2009**, *35*, 167.
5. Denlinger, C. E.; Rundall, B. K.; Jones, D. R. *Semin. Thorac. Cardiovasc. Surg.* **2004**, *16*, 28.
6. D'Amico, T. A.; Harpole, D. H., Jr. *Chest Surg. Clin. N. Am.* **2000**, *10*, 451.
7. Savage, P.; Stebbing, J.; Bower, M.; Crook, T. *Nat. Clin. Pract. Oncol.* **2009**, *6*, 43.
8. Wilson, T. R.; Johnston, P. G.; Longley, D. B. *Curr. Cancer Drug Targets* **2009**, *9*, 307.
9. Cragg, G. M.; Grothaus, P. G.; Newman, D. J. *Chem. Rev.* **2009**, *109*, 3012.
10. Smyrniotopoulos, V.; Vagias, C.; Roussis, V. *Mar. Drugs* **2009**, *7*, 184. and references cited therein.
11. Etahiri, S.; Bultel-Poncé, V.; Caux, C.; Guyot, M. *J. Nat. Prod.* **2001**, *64*, 1024. and references cited therein.
12. Kontiza, I.; Stavri, M.; Zloh, M.; Vagias, C.; Gibbons, S.; Roussis, V. *Tetrahedron* **2008**, *64*, 1696.
13. Kladi, M.; Vagias, C.; Papazafiri, P.; Brogi, S.; Tafi, A.; Roussis, V. *J. Nat. Prod.* **2009**, *72*, 190.
14. Bavoso, A.; Cafieri, F.; De Napoli, L.; Di Blasio, B.; Fattorusso, E.; Pavone, C.; Santacroce, C. *Gazz. Chim. Ital.* **1987**, *117*, 87.
15. Seco, J. M.; Quiñoá, E.; Riguera, R. *Chem. Rev.* **2004**, *104*, 17.
16. Cafieri, F.; Fattorusso, E.; Santacroce, C. *Tetrahedron Lett.* **1984**, *25*, 3141.
17. Smyrniotopoulos, V.; Quesada, A.; Vagias, C.; Moreau, D.; Roussakis, C.; Roussis, V. *Tetrahedron* **2008**, *64*, 5184.
18. Fenical, W.; Finer, J.; Clardy, J. *Tetrahedron Lett.* **1976**, *17*, 731.
19. De Rosa, S.; De Stefano, S.; Scarpelli, P.; Zavodnik, N. *Phytochemistry* **1988**, *27*, 1875.
20. Fattorusso, E.; Magno, S.; Santacroce, C.; Sica, D.; Di Blasio, B.; Pedone, C.; Impellizzeri, G.; Mangiafico, S.; Oriente, G.; Piattelli, M.; Scinto, S. *Gazz. Chim. Ital.* **1976**, *106*, 779.
21. Cafieri, F.; Ciminiello, P.; Fattorusso, E.; Mangoni, C. *Gazz. Chim. Ital.* **1990**, *120*, 139.
22. Cafieri, F.; Ciminiello, P.; Fattorusso, E.; Santacroce, C. *Experientia* **1982**, *38*, 298.
23. Cafieri, F.; De Napoli, L.; Fattorusso, E.; Santacroce, C. *Phytochemistry* **1987**, *26*, 471.
24. Cafieri, F.; De Napoli, L.; Fattorusso, E.; Impellizzeri, G.; Piattelli, M. *Experientia* **1977**, *33*, 1549.
25. Smyrniotopoulos, V.; Vagias, C.; Rahman, M. M.; Gibbons, S.; Roussis, V. *Chem. Biodiversity*, in press. doi:10.1002/cbdv.200800309.
26. Smyrniotopoulos, V.; Vagias, C.; Rahman, M. M.; Gibbons, S.; Roussis, V. *J. Nat. Prod.* **2008**, *71*, 1386.
27. Cafieri, F.; Ciminiello, P.; Santacroce, C.; Fattorusso, E. *Phytochemistry* **1982**, *21*, 2412.
28. Cafieri, F.; Fattorusso, E.; Mayol, L.; Santacroce, C. *Tetrahedron* **1986**, *42*, 4273.
29. Brady, S. F.; Bondi, S. M.; Clardy, J. *J. Am. Chem. Soc.* **2001**, *123*, 9900.
30. Brady, S. F.; Singh, M. P.; Janso, J. E.; Clardy, J. *J. Am. Chem. Soc.* **2000**, *122*, 2116.
31. Kettering, M.; Valdivia, C.; Sterner, O.; Anke, H.; Thines, E. *J. Antibiot.* **2005**, *58*, 390.
32. Valdivia, C.; Kettering, M.; Anke, H.; Thines, E.; Sterner, O. *Tetrahedron* **2005**, *61*, 9527.

33. Ingrassia, L.; Lefranc, F.; Dewelle, J.; Pottier, L.; Mathieu, V.; Spiegl-Kreinecker, S.; Sauvage, S.; El Yazidi, M.; Dehoux, M.; Berger, W.; Van Quaquebeke, E.; Kiss, R. *J. Med. Chem.* **2009**, *52*, 1100.
34. Lefranc, F.; Mijatovic, T.; Kondo, Y.; Sauvage, S.; Roland, I.; Debeir, O.; Krstic, D.; Vasic, V.; Gailly, P.; Kondo, S.; Blanco, G.; Kiss, R. *Neurosurgery* **2008**, *62*, 211.
35. Mijatovic, T.; Mathieu, V.; Gaussin, J. F.; De Neve, N.; Ribaucour, F.; Van Quaquebeke, E.; Dumont, P.; Darro, F.; Kiss, R. *Neoplasia* **2006**, *8*, 402.
36. Mathieu, V.; Pirker, C.; Martin de Lassalle, E.; Vernier, M.; Mijatovic, T.; De Nève, N.; Gaussin, J. F.; Dehoux, M.; Lefranc, F.; Berger, W.; Kiss, R. *J. Cell. Mol. Med.*, in press. doi:10.1111/j.1582-4934.2009.00708.x.
37. Bruyère, C.; Mijatovic, T.; De Nève, N.; Gaussin, J. F.; Gras, T.; Nindfa, P.; Dehoux, M.; Saussez, S.; Kiss, R. In: Proceedings of the 100th Annual Meeting of the American Association for Cancer Research. Abstract no. 4135. Denver, Philadelphia, April 18–22, 2009.
38. Dumont, P.; Ingrassia, L.; Rouzeau, S.; Ribaucour, F.; Thomas, S.; Roland, I.; Darro, F.; Lefranc, F.; Kiss, R. *Neoplasia* **2007**, *9*, 766.
39. Yao, Y.; Jia, X. Y.; Tian, H. Y.; Jiang, Y. X.; Xu, G. J.; Qian, Q. J.; Zhao, F. K. *Biochim. Biophys. Acta* **2009**, *1794*, 1433.
40. Van Quaquebeke, E.; Mahieu, T.; Dumont, P.; Dewelle, J.; Ribaucour, F.; Simon, G.; Sauvage, S.; Gaussin, J. F.; Tuti, J.; El Yazidi, M.; Van Vynckt, F.; Mijatovic, T.; Lefranc, F.; Darro, F.; Kiss, R. *J. Med. Chem.* **2007**, *50*, 4122.
41. Lamoral-Theys, D.; Andolfi, A.; Van Goietsenoven, G.; Cimmino, A.; Le Calvé, B.; Wauthoz, N.; Mégalizzi, V.; Gras, T.; Bruyère, C.; Dubois, J.; Mathieu, V.; Kornienko, A.; Kiss, R.; Evidente, A. *J. Med. Chem.* **2009**, *52*, 6244.
42. De Hauwer, C.; Camby, I.; Darro, F.; Migeotte, I.; Decaestecker, C.; Verbeek, C.; Danguy, A.; Pasteels, J. L.; Brotchi, J.; Salmon, I.; Van Ham, P.; Kiss, R. *J. Neurobiol.* **1998**, *37*, 373.
43. Delbrouck, C.; Doyen, I.; Belot, N.; Decaestecker, C.; Ghanooni, R.; de Lavareille, A.; Kaltner, H.; Choufani, G.; Danguy, A.; Vandenhoven, G.; Gabius, H. J.; Hassid, S.; Kiss, R. *Lab. Invest.* **2002**, *82*, 147.
44. Suarez, Y.; Gonzalez, L.; Cuadrado, A.; Berciano, M.; Lafarga, M.; Munoz, A. *Mol. Cancer Ther.* **2003**, *2*, 863.
45. Sewell, J. M.; Mayer, I.; Langdon, S. P.; Smyth, J. F.; Jodrell, D. I.; Guichard, S. M. *Eur. J. Cancer* **2005**, *41*, 1637.
46. Janmaat, M. L.; Rodriguez, J. A.; Jimeno, J.; Krut, F. A.; Giaccone, G. *Mol. Pharmacol.* **2005**, *68*, 502.
47. Jimenez, J. C.; Lopez-Macia, A.; Gracia, C.; Varon, S.; Carrascal, M.; Caba, J. M.; Royo, M.; Francesch, A. M.; Cuevas, C.; Giralt, E.; Albericio, F. *J. Med. Chem.* **2008**, *51*, 4920.